

Design and Characterization of a Low-Cost Piezoelectric Vibration Energy Harvester with Bulk PZT Film

TIAN Xingyao, HE Xuefeng

(Key Laboratory of Optoelectronic Technology and Systems of the Education Ministry of China,
Chongqing University, Chongqing 400044, China)

Abstract: To improve the efficiency of MEMS piezoelectric vibration energy harvesters (PVEHs), the bulk lead zirconate titanate (PZT) has been used to substitute the thin film PZT for the higher mechanical-electrical coupling coefficients. The expensive equipment of micromachining set a high entry barrier on the research of PVEHs with high efficiency. To solve this issue, this paper developed an efficient PVEH with bulk PZT using common precision machining, whose dimensions and electrical outputs are comparable to the MEMS devices. After numerically analyzing the effects of the length ratio of the proof mass to the harvester on the output power, a compact PVEH consisting of a cantilevered uni-morph and a tungsten proof mass was designed. Simulations show that the mechanical damping ratio and the thickness have little effects on the optimized length ratio. By using a uni-morph with the copper structural layer of about 80-90 μm and the bulk PZT-5H layer of 139 μm , a low-cost harvester prototype was assembled. The key parameters of the prototype were experimentally identified and compared with the theoretical predictions. Under the harmonic base excitation of 0.4g (where $g = 9.8\text{m/s}^2$) at 160 Hz, the maximum output power of the prototype is about 76.7 μW , with the normalized power density of about 3.35 $\text{mW/cm}^3/\text{g}^2$. Under base excitation of 0.4g at 159Hz, the prototype charged a 680 μF capacitor from 0 to 4.84V in about 154 seconds.

Key words: Energy Harvesting; Vibration; Piezoelectricity; Bulk Lead Zirconate Titanate; Precision Machining

1 Introduction

Vibration energy harvesters (VEHs) converting ambient vibrations into electricity receive growing attention in recent years. Compared with traditional chemical batteries, VEHs possess such advantages as long lives, maintenance-free and pollution-free, making them good substitutes of batteries as the power sources of wireless sensor nodes. A large number of piezoelectric^[1-6], electrostatic^[7, 8], electromagnetic^[9, 10], and triboelectric^[11, 12] VEHs have been developed. Among these harvesters, the piezoelectric vibration energy harvesters (PVEHs) attract most attention for the simple structure, easiness of miniaturization and high power density^[13-15].

Micromachining has been used to fabricate MEMS PVEHs to reduce the volume and improve the power density^[16]. By using aluminum nitride (AlN) as the piezoelectric film and silicon as the proof mass, Andosca et al.^[17] developed a PVEH of

6mm \times 8.375mm using a standard micromachining process, which produced a peak power of 32 μW under 0.5g (where $g = 9.8\text{m/s}^2$) at 58 Hz, with the normalized power density (NPD) of 9.039 $\text{mW/cm}^3/\text{g}^2$. As the mechanical-electrical coupling coefficients of the bulk piezoelectric materials are much higher than those of the thin films, bulk lead zirconate titanate (PZT) film have been used to improve the electrical output of PVEHs recently^[18-24]. Aktakka et al.^[18] developed the first MEMS energy harvester integrating a bulk PZT piezoelectric layer by using a process involving aligned solder-bonding and thinning of bulk PZT pieces on silicon. The device with a silicon proof mass generates 0.15 μW output under 0.1g at 263Hz, with NPD of 1.215 $\text{mW/cm}^3/\text{g}^2$. Then, the output performance was greatly improved by using tungsten to substitute silicon as the proof mass^[19]. A harvester with the size of 7mm \times 7mm produces 2.74 μW under 0.1 g at 167 Hz, and

205 μ W under 1.5g at 154 Hz, with NPD of 10.148mW/cm³/g². Janphuang et al.^[21] reported a process to fabricate MEMS PVEH with bulk PZT layer. The experimental NPD of a device with the area of 11.5mm \times 10.8mm is 3.346mW/cm³/g² under the base excitation of 0.1g at 100Hz.

The fabrication of MEMS PVEHs based on the bulk PZT film requires expensive micromachining equipment, which sets a high entry barrier on the studies of the efficient PVEHs. Noting that the lengths and widths of these MEMS PVEHs are about several millimeters, which can also be fabricated by the precision machining, this paper designed a cantilevered PVEH which may be fabricated by assembling a commercially available bulk PZT composite beam with a tungsten proof mass. A harvester prototype was fabricated and the experimental results demonstrated that the low-cost and efficient PVEHs can be fabricated by common precision machining.

2 Device Optimization

2.1 Modeling of Cantilevered Piezoelectric Vibration Energy Harvester

APVEH mainly consists of a proof mass and a piezoelectric cantilever, as shown in Fig. 1. The proof mass is fixed at the tip end of the cantilever. Here, the cantilever is a uni-morph with a bulk PZT piezoelectric layer on a copper structural layer. The distribute-parameter models will be used to optimize the structure of this type of harvesters. The length and width of the cantilever are L_b and W_b , the thicknesses of the PZT and copper layers are h_p and h_s , and the length, width and thickness of the proof mass are L_m , W_m and H_m , respectively. For the harvester, the total length L (which is the sum of L_b and L_m , i.e. $L = L_b + L_m$) is set as a fixed value in the optimization. The base excitation is in the y direction, denoted by $w_b(t)$. The deflection of the cross section with the coordinate of x is denoted by $w(x, t)$. It is assumed that there are two electrodes on the upper and bottom surfaces of the PZT layer for $0 \leq x \leq L_e$. As a result, only the PZT layer

near the clamped end of cantilever with $0 \leq x \leq L_e$ produces electricity under base excitations.

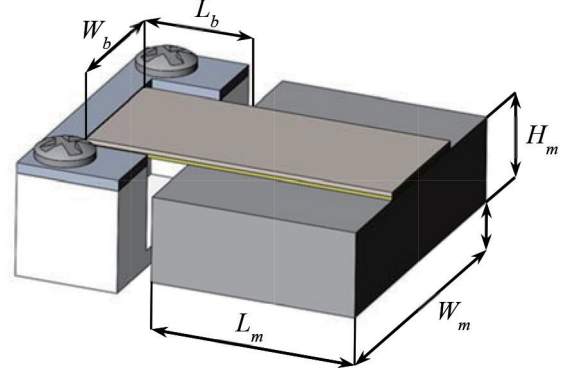


Fig. 1 Schematic of a Cantilevered Piezoelectric Energy Harvester

For the cantilevered PVEHs, the responses can be approximated by the first mode^[25]. In this case, the deflection of the cantilever can be expressed as^[25-29]

$$w(x, t) = \varphi(x) \eta(t), \quad (1)$$

where $\varphi(x)$ and $\eta(t)$ are, respectively, the mode shape and modal coordinate of the first mode. Here, the mode shape $\varphi(x)$ has been normalized by letting the modal mass equal to unit. The first undamped natural frequency of the beam is^[25, 28, 29]

$$\omega_n = \lambda^2 \sqrt{\frac{YI}{m L_b^4}}, \quad (2)$$

where m is the mass per unit length of the cantilever, YI is the bending stiffness, and λ is the eigenvalue which can be obtained by solving the characteristic equation of the harvester.

Considering the effect of the piezoelectric layer, the equation of motion of the harvester can be expressed as

$$\ddot{\eta}(t) + 2\zeta_r \omega_n \dot{\eta}(t) + \omega_n^2 \eta(t) + \chi v(t) = f(t), \quad (3)$$

where ζ_r is the mechanical damping ratio and $v(t)$ is the voltage between two electrodes of the piezoelectric layer. The coupling coefficient and the modal force are, respectively, given by

$$\chi = -\frac{\bar{e}_{31} W_b}{h_p} \varphi'(L_b) \int_{h_p} y dy, \quad (4)$$

and

$$f(t) = -\ddot{w}_b(t) \begin{bmatrix} m \int_0^{L_b} \varphi(x) dx + M_t \varphi(L_b) \\ + 0.5 L_m M_t \varphi'(L_b) \end{bmatrix}, \quad (5)$$

where \bar{e}_{31} is the piezoelectric constant of bulk PZT.

When an electrical resistance R is connected with two electrodes of piezoelectric layer, the coupled circuit equation of the harvester is given by^[25, 27-29]

$$C_p \dot{v}(t) + \frac{v(t)}{R} - k\eta(t) = 0, \quad (6)$$

where C_p is the capacitance of the piezoelectric

$$V = \frac{j2\omega Rk \left[m \int_0^{L_b} \varphi(x) dx + M_t \varphi(L_b) + 0.5 L_m M_t \varphi'(L_b) \right] A_0}{a(\omega) (2 + j2\omega RC_p) + 2\omega Rk}, \quad (9)$$

where

$$a(\omega) = \omega_n^2 - \omega^2 + j2\zeta_r \omega_n \omega. \quad (10)$$

The output power of the harvesters is

$$P = \frac{V^2}{2R}. \quad (11)$$

2.2 Structural Optimization

By using a lumped-parameter model, He et al. optimized the geometries of a MEMS PVEH^[30]. In the following, a PVEH which can be fabricated using the precision machining will be designed using the distributed-parameter model. The uni-morph copper reinforce PZT-5H^[31] was used as the cantilever. To assemble the device into space with the size of 1cm×1cm×0.3cm, the total length of the harvester is set as $L = 9000\mu\text{m}$, the width of the cantilever is $W_b = 4000\mu\text{m}$, and the width and thickness of the proof mass are $W_m = 9000\mu\text{m}$ and $H_m = 2500\mu\text{m}$, respectively. The thicknesses of the PZT-5H and the copper layers are $h_p = 139\mu\text{m}$ and $h_s = 102\mu\text{m}$, the same with those of the T216-H4-203Y bimorphs from Piezo systems Inc. The Young's modulus, piezoelectric constant and the permittivity component at a constant strain of PZT-5H are $Y_p = 60.6\text{GPa}$, $e_{31} = -16.6\text{C/m}^2$ and $\bar{\epsilon}_{33}^S = 25.6 \times 10^{-9} \text{F/m}$ ^[31]. The

layer, given by

$$C_p = \frac{\bar{\epsilon}_{33}^S W_b L_e}{h_p}, \quad (7)$$

where $\bar{\epsilon}_{33}^S$ is the permittivity component at constant strain. The parameter k can be written as

$$k = -\bar{e}_{31} h_{pc} W_b \varphi'(L_b), \quad (8)$$

where h_{pc} is the distance from the center of the PZT layer to the neutral axis.

Under a harmonic base excitation with the acceleration of $\ddot{w}_b(t) = A_0 \sin \omega t$, the voltage across the resistance is also a harmonic function of time t , with the amplitude given by

Young's modulus of the copper is $Y_s = 100\text{GPa}$. The proof mass is made of tungsten, with the density of $19.26 \times 10^3 \text{kg/m}^3$. The base acceleration amplitude was set at 0.4g in the optimization.

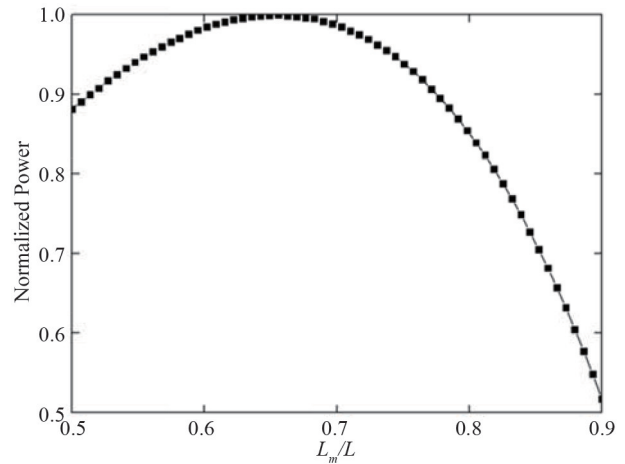


Fig. 2 Normalized Powers Versus Length Ratio of Proof Mass to Harvester

He et al. have analyzed the effect of the length ratio L_e/L_b on the output power^[30]. They concluded that when the length ratio L_m/L is larger than 0.5, the optimized length ratio L_e/L_b is 1, which means that the electrode should occupy all the surface of cantilever when the length of the proof mass is longer than the cantilever. By using the distributed-parameter

model, the same conclusion is obtained. By setting $L_e/L_b = 1$, when the electrical resistance changes from $1k\Omega$ to $1000k\Omega$, the simulated maximum normalized output power versus the length ratio L_m/L is plotted in Fig.2. When L_m/L increased from 0.5 to 1, the maximum normalized output power increases firstly and then decreases. The output power reaches the maximum when the length ratio L_m/L is about 0.66.

The thickness of the structural layer affects the stiffness of the cantilever and output power. When the thickness of the structural layer increased from 60 to $120\mu m$, the normalized power was simulated, as shown in Fig. 3. For the harvesters with different structural layer thicknesses, the relationships between the normalized power and the length ratio L_m/L are similar and the maximum normalized power occurs at about $L_m/L = 0.66$. Therefore, when the total length of the harvester is fixed, the thickness of the structural layer has little effects on the optimized length of the proof mass. Under the base excitation of 0.4g, the optimized thickness of the structural layer is between 80 and $90\mu m$.

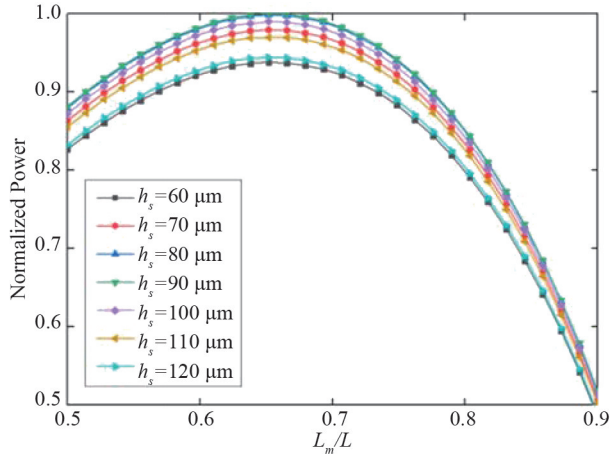


Fig. 3 Normalized Power Versus Length Ratio of Proof Mass to Harvester for Different Structural Layer Thicknesses

The mechanical damping ratio greatly affects the output power of PVEHs^[32]. For the cases with different mechanical damping ratios from 0.025 to 0.045, the simulated normalized output power versus

the length ratio L_m/L is given in Fig. 4. As expected, the output power strongly depends on the mechanical damping ratio. But when the mechanical damping ratio changed, the optimized L_m/L is the same, with a value of about 0.66. As a result, the mechanical damping ratio has little influence on the optimization of the geometries of the PVEHs.

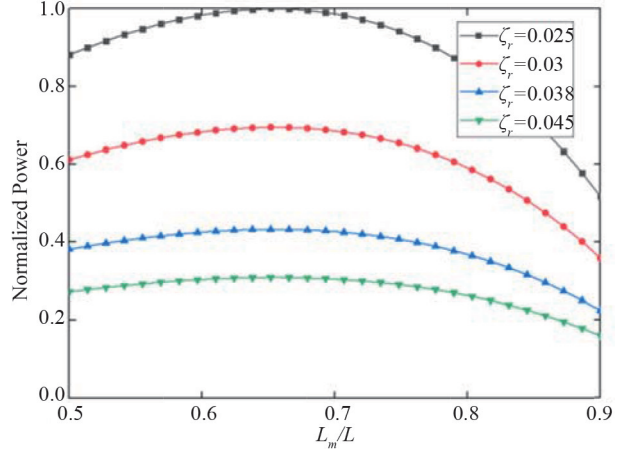


Fig. 4 Normalized Power Versus Length Ratio of Proof Mass to Harvester for Different Mechanical Damping

As a result, the optimized geometrical parameters are mainly determined by the length ratio L_m/L and the length ratio L_e/L_b . The thickness of the structural layer and the mechanical damping ratio has little effects on the optimization of the lengths of the cantilever, the proof mass and the electrode. The optimized geometrical parameters are listed in Table 1.

Table 1 Optimized Geometrical Parameters

Geometrical Parameter (unit)	Value
Cantilever Length $L_b(\mu m)$	3000
Cantilever Width $W_b(\mu m)$	4000
Piezoelectric Layer Thickness $h_p(\mu m)$	139
Structure Layer Thickness $h_s(\mu m)$	80-90
Electrode Length $L_e(\mu m)$	3000
Proof Mass Length $L_m(\mu m)$	6000
Proof Mass Width $W_m(\mu m)$	9000
Proof Mass Thickness $H_m(\mu m)$	2500

3 Parameter Identification

A harvester prototype with the parameters listed in Table 1 was fabricated. The total volume of the device is about 0.143cm^3 . The prototype was fixed onto an electromagnetic shaker, as shown in Fig. 5. A sinusoidal voltage signal produced by an oscilloscope was enlarged by a power amplifier to drive the shaker. Acceleration of the shaker was monitored by an accelerometer and the output voltage of the harvester was measured by the oscilloscope.

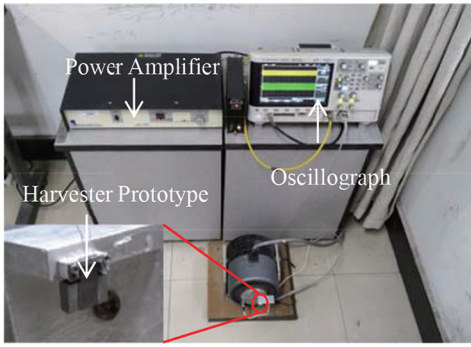


Fig. 5 Experimental Setup

The key parameters of the prototype, including the first natural frequency ω_n , the mechanical damping ratio ζ_r , the capacitance C_p and the electromechanical coupling term χ , were identified by experiments^[33]. The short-circuit resonant frequency ω_{sc} and open-circuit resonant frequency ω_{oc} were firstly obtained by connecting resistors of $1\text{k}\Omega$ and $10\text{M}\Omega$, with the harvester, respectively. The capacitance C_p was measured using an impedance analyzer.

The effective damping ratio ζ_{eff} is the sum of the mechanical damping ratio ζ_r and electrical damping ratio ζ_{el} ^[33], given by

$$\zeta_{eff} = \zeta_r + \zeta_{el}, \quad (12)$$

The electrical damping ratio can be expressed as [33]

$$\zeta_{el} = \frac{v^2 \sigma_{el}}{\sigma_{el}^2 + (1 - \gamma^2)^2}, \quad (13)$$

where

$$\gamma^2 = 1 - \frac{\omega_{sc}^2}{\omega_{oc}^2}, \quad (14)$$

and

$$\sigma_{el} = \frac{1}{\omega_n C_p R}. \quad (15)$$

Therefore, the mechanical damping ratio ζ_r can be obtained after the effective damping ratio ζ_{eff} has been measured. The effective damping ratio ζ_{eff} can be identified using exponentially decaying voltage amplitudes^[34].

The mechanical damping ratio and electromechanical coupling term affect resonant frequency^[35, 36]. As the prototype is a strongly coupled and lightly damped energy harvester^[37], it is easy to distinguish short-circuit and open circuit resonant frequencies by experiments. The electromechanical coupling term can be approximately expressed as^[38]

$$\chi = \omega_n \sqrt{\left(\frac{\omega_{oc}^2}{\omega_{sc}^2} - 1\right) C_p}. \quad (16)$$

The parameters of the prototype were experimentally identified using the above methods. The theoretical and measured parameters were listed in Table 2. As there is a thin layer of epoxy ($<20\mu\text{m}$) between the copper layer and the PZT-5H layer, it is difficult to precisely determine the thickness of the structural layer, which may cause the errors between the theoretical and experimental parameters.

Table 2 Theoretical and Experimental Parameters of the Prototype

Parameters	Theoretical ($h_s = 80\mu\text{m}$)	Theoretical ($h_s = 90\mu\text{m}$)	Measured
Natural Frequency ω_n (Hz)	187.0	200.0	156.2
Open-Circuit Frequency ω_{oc} (Hz)	191.3	204.8	160
Capacitance C_p (nF)	2.94	2.94	2.75
Mechanical Damping Ratio ζ_r	-	-	0.03778
Electromechanical Coupling Constant χ (N/V)	0.01374	0.01523	0.01142

4 Experimental Results and Discussions

4.1 Output Performance Characterization

Under base excitation of 0.4g, the experimental root-mean-square (RMS) open-circuit voltage versus the excitation frequency was given in Fig. 6. The open-circuit resonance frequency is about 160Hz, with the maximum RMS open-circuit voltage of about 7.81V. Then, by fixing the excitation frequency at 160 Hz, the RMS voltage across resistors with different resistances was measured and the output power was calculated from Eq. (11), as shown in Fig. 7. The matched resistance is about 260k Ω at the open-circuit resonance frequency. When the excitation frequency is 160Hz, the experimental maximum output power is about 76.7 μ W. The normalized maximum power density is about 3.35mW/cm³/g², comparable with the MEMS PVEHs with the bulk PZT as the piezoelectric layer^[21].

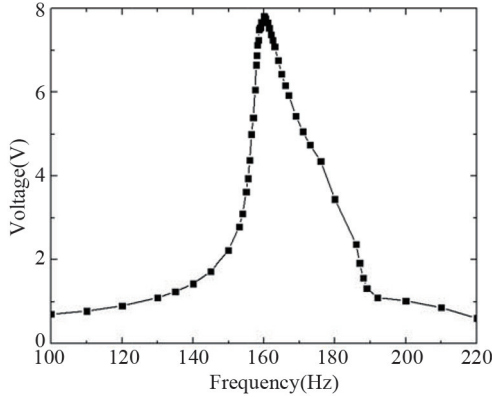


Fig. 6 RMS Open-Circuit Voltage Versus Frequency Under 0.4 g

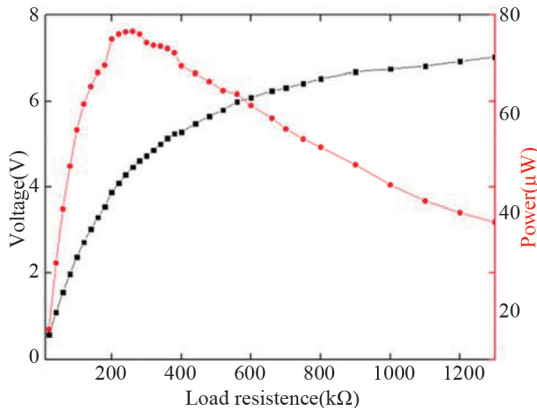


Fig. 7 Voltage and Power Versus Electrical Resistance at Anti-Resonance Frequency Under 0.4g

4.2 Charging Experiments

Under the base excitation of 0.4g, by using the harvester to charge a capacitor of 680 μ F from 0 to 4.84V through the power management circuit reported in Reference^[39], the experimental charging time at different excitation frequencies was recorded, as shown in Fig.8. The charging time decreases firstly and then increases, with the shortest charging time of 154 seconds at 159Hz.

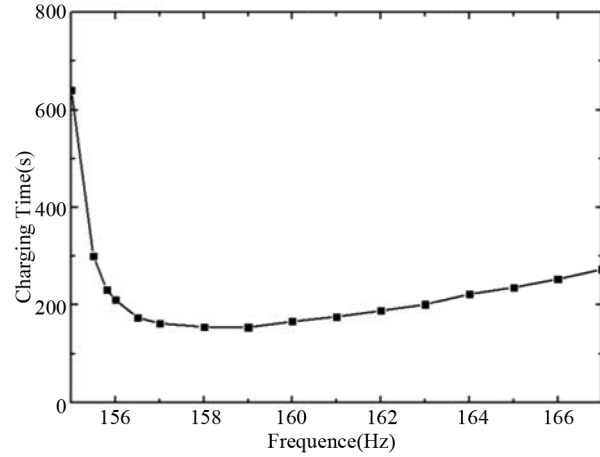


Fig. 8 Charging Time Versus Excitation Frequency

5 Conclusions

Efficient PVEHs with bulk PZT may be fabricated by MEMS technology. But the expensive equipment of the micromachining limit the extensive studies of these devices. Therefore, it is of significance to using precision machining to fabricate the PVEHs with bulk PZT layer. By using a distributed-parameter model, a cantilevered PVEH, which may be fabricated by assembling a commercially available bulk PZT composite beam with a tungsten proof mass, was designed. The optimal ratio of the length of the proof mass to that of the harvester is about 0.66. The mechanical damping ratio and the thickness of the structural layer have little effects on the optimal length ratio. A harvester prototype was fabricated using common precision machining and tested. The first natural frequency, mechanical damping ratio, the capacitance and the electromechanical coupling term were experimentally identified. The experimen-

tal short-circuit and open-circuit resonant frequencies are about 156.2 and 160Hz, respectively. Under the harmonic base excitation of 0.4g at 160Hz, the output power across a matched resistance of 260k Ω is about 76.7 μ W, with the normalized power density of about 3.35mW/cm³/g², which is comparable to MEMS PVEHs. The shortest time to charge a capacitor of 680 μ F from 0 to 4.84V is about 154 seconds. By thinning the bulk PZT and the copper films using such machining process as mechanical grinding, the output performance may be further improved.

ACKNOWLEDGMENT

This work was financially supported by the National Natural Science Foundation of China (Nos. 61774026 and 61376116).

References

- [1] Roundy S. and Wright P.K. (2004). A piezoelectric vibration based generator for wireless electronics. *Smart Materials and Structures*, 13(5), pp. 1131-1142.
- [2] Erturk A. and Inman D.J. (2009). An experimentally validated bimorph cantilever model for piezoelectric energy harvesting from base excitations. *Smart Materials and Structures*, 18(2), 025009.
- [3] Adhikari S., Friswell M.I. and Inman D.J. (2009). Piezoelectric energy harvesting from broadband random vibrations. *Smart Materials and Structures*, 18(11), 115005.
- [4] Ferrari M., Baù M., Guizzetti M. and Ferrari V. (2011). A single-magnet nonlinear piezoelectric converter for enhanced energy harvesting from random vibrations. *Sensors and Actuators A: Physical*, 172(1), pp. 287-292.
- [5] Muthalif A.G.A. and Nordin N.H.D. (2015). Optimal piezoelectric beam shape for single and broadband vibration energy harvesting: Modeling, simulation and experimental results. *Mechanical Systems and Signal Processing*, 54-55, pp. 417-426.
- [6] Fan K., Tan Q., Zhang Y., Liu S., Cai M. and Zhu Y. (2018). A monostable piezoelectric energy harvester for broadband low-level excitations. *Applied Physics Letters*, 112(12), 123901.
- [7] Le C.P. and Halvorsen E. (2012). MEMS electrostatic energy harvesters with end-stop effects. *Journal of Micromechanics and Microengineering*, 22(7), 074013.
- [8] Perez M., Boisseau S., Gasnier P., Willemin J., Geisler M. and Reboud J.L. (2016). A cm scale electret-based electrostatic wind turbine for low-speed energy harvesting applications. *Smart Materials and Structures*, 25(4), 045015.
- [9] Sari I., Balkan T. and Külah H. (2010). An Electromagnetic Micro Power Generator for Low-Frequency Environmental Vibrations Based on the Frequency Upconversion Technique. *Journal of Microelectromechanical Systems*, 19(1), pp. 14-27.
- [10] Halim M.A., Rantz R., Zhang Q., Gu L., Yang K. and Roundy S. (2018). An electromagnetic rotational energy harvester using sprung eccentric rotor, driven by pseudo-walking motion. *Applied Energy*, 217, pp. 66-74.
- [11] Lin L., Wang S., Xie Y., Jing Q., Niu S., Hu Y. and Wang Z.L. (2013). Segmentally structured disk triboelectric nanogenerator for harvesting rotational mechanical energy. *Nano Lett*, 13(6), pp. 2916-2923.
- [12] Chen B., Yang Y. and Wang Z.L. (2018). Scavenging Wind Energy by Triboelectric Nanogenerators. *Advanced Energy Materials*, 8(10), 1702649.
- [13] Anton S.R. and Sodano H.A. (2007). A review of power harvesting using piezoelectric materials (2003 - 2006). *Smart Materials and Structures*, 16(3), pp. R1-R21.
- [14] Niell G.E., Alex A.E. and Myron S. (2001). A self-powered mechanical strain energy sensor. *Smart Materials and Structures*, 10(2), pp. 293-299.
- [15] Keshmiri A., Wu N. and Wang Q. (2018). A new nonlinearly tapered FGM piezoelectric energy harvester. *Engineering Structures*, 173, pp. 52-60.
- [16] Todaro M.T., Guido F., Mastronardi V., Desmaele D., Epifani G., Algieri L. and De Vittorio M. (2017). Piezoelectric MEMS vibrational energy harvesters: Advances and outlook. *Microelectronic Engineering*, 183-184, pp. 23-36.
- [17] Andosca R., McDonald T.G., Genova V., Rosenberg S., Keating J., Benedixen C. and Wu J. (2012). Experimental and theoretical studies on MEMS piezoelectric vibrational energy harvesters with mass load-

- ing. *Sensors and Actuators A: Physical*, 178, pp. 76-87.
- [18] Aktakka E.E., Peterson R.L. and Najafi K. (2010). A CMOS-compatible piezoelectric vibration energy scavenger based on the integration of bulk PZT films on silicon. In: 2010 *International Electron Devices Meeting*. San Francisco: IEEE, pp. 716-719.
- [19] Aktakka E.E., Peterson R. and Najafi K. (2011). Thinned-PZT on SOI process and design optimization for piezoelectric inertial energy harvesting. In: *Solid-State Sensors, Actuators and Microsystems Conference (TRANSDUCERS)*, 2011 16th International. Beijing: IEEE, pp. 1649-1652.
- [20] Janphuang P., Lockhart R., Briand D. and De Rooij N.F. (2012). Wafer Level Fabrication of Vibrational Energy Harvesters using Bulk PZT Sheets. *Procedia Engineering*, 47, pp. 1041-1044.
- [21] Janphuang P., Lockhart R., Uffer N., Briand D. and De Rooij N.F. (2014). Vibrational piezoelectric energy harvesters based on thinned bulk PZT sheets fabricated at the wafer level. *Sensors and Actuators A: Physical*, 210, pp. 1-9.
- [22] Quintero A.V., Besse N., Janphuang P., Lockhart R., Briand D. and De Rooij N.F. (2014). Design optimization of vibration energy harvesters fabricated by lamination of thinned bulk-PZT on polymeric substrates. *Smart Materials and Structures*, 23 (4), 045041.
- [23] Yi Z.R., Yang B., Li G.M., Liu J.Q., Chen X., Wang X.L. and Yang C.S. (2017). High performance bimorph piezoelectric MEMS harvester via bulk PZT thick films on thin beryllium-bronze substrate. *Applied Physics Letters*, 111(1), 013902.
- [24] Tian Y.W., Li G.M., Yi Z.R., Liu Z.Q. and Yang B. (2018). A low-frequency MEMS piezoelectric energy harvester with a rectangular hole based on bulk PZT film. *Journal of Physics and Chemistry of Solids*, 117, pp. 21-27.
- [25] Erturk A. and Inman D.J. (2008). A Distributed Parameter Electromechanical Model for Cantilevered Piezoelectric Energy Harvesters. *Journal of Vibration and Acoustics*, 130(4), 041002.
- [26] Ge S. S., Lee T. H., Zhu G. and Hong F. (2001). Variable structure control of a distributed-parameter flexible beam. *Journal of Robotic Systems*, 18(1), pp. 17-27.
- [27] He X.F., Du Z.G., Zhao X.Q., Wen Z.Y. and Yin X.F. (2011). Modeling and experimental verification for cantilevered piezoelectric vibration energy harvester. *Optics and Precision Engineering*, 19(8), pp. 1771-1778. (In Chinese)
- [28] Erturk A. and Inman D.J. (2011). *Piezoelectric Energy Harvesting*. United Kingdom: John Wiley & Sons, Ltd.
- [29] Patel R., McWilliam S. and Popov A.A. (2011). A geometric parameter study of piezoelectric coverage on a rectangular cantilever energy harvester. *Smart Materials and Structures*, 20(8), 085004.
- [30] He X.F., Shang Z.G., Cheng Y.Q. and Zhu Y. (2013). A micromachined low-frequency piezoelectric harvester for vibration and wind energy scavenging. *Journal of Micromechanics and Microengineering*, 23(12), 125009.
- [31] Piezo.com (2018), Material Properties - Piezo Support Date. [online] Available at: <https://support.piezo.com/article/62-material-properties> [Accessed; 20 Dec. 2018].
- [32] Erturk A., Anton S.R., Bilgen O. and Inman D.J. (2009). Effect of Material Constants and Mechanical Damping on Piezoelectric Power Generation. In: *International Design Engineering Technical Conferences and Computers and Information in Engineering Conference*. San Diego: ASME, pp. 513-522.
- [33] Goldschmidtboeing F., Wischke M., Eichhorn C. and Woias P. (2011). Parameter identification for resonant piezoelectric energy harvesters in the low- and high-coupling regimes. *Journal of Micromechanics and Microengineering*, 21(4), 045006.
- [34] Gross D., Hauger W., Schröder J., Wall W.A. and Govindjee S. (2011). *Engineering Mechanics 3: Dynamics*. Heidelberg: Springer-Verlag Berlin Heidelberg.
- [35] Renno J.M., Daqaq M.F. and Inman D.J. (2009). On the optimal energy harvesting from a vibration source. *Journal of Sound and Vibration*, 320(1-2), pp. 386-405.
- [36] Liao Y.B. and Sodano H.A. (2008). Model of a single mode energy harvester and properties for optimal power generation. *Smart Materials and Structures*, 17(6), 065026.
- [37] Erturk A. and Inman D.J. (2011). Parameter identification and optimization in piezoelectric energy harvesters.

ting: analytical relations, asymptotic analyses, and experimental validations. *Proceedings of the Institution of Mechanical Engineers, Part I: Journal of Systems and Control Engineering*, 225(4), pp. 485-496.

- [38] Shu Y.C. and Lien I.C. (2006). Analysis of power output for piezoelectric energy harvesting systems. *Smart Materials and Structures*, 15(6), pp. 1499-1512.
- [39] Zhang C., He X.F., Li S.Y., Cheng Y.Q. and Rao Y. (2015). A wind energy powered wireless temperature sensor node. *Sensors (Basel)*, 15(3), pp. 5020-5031.

Authors' Biographies



TIAN Xingyao is currently pursuing his Master degree in the College of Optoelectronic Engineering at Chongqing University. He is interested in the piezoelectric kinetic energy harvesters.
Email: tianxingyao@163.cm



HE Xuefeng received his received his Ph.D. degree in Engineering Mechanics from Peking University, China, in 2005. He is currently a professor of Chongqing University, China. His research interests include Micro/Nanofabrication processes, power MEMS and

wireless sensor networks.

Email: hexuefeng@cqu.edu.cn